Human Molecular Genetics, 2009, Vol. 18, No. 10 **1769–1778**
doi:10.1093/hmg/ddp089
Advance Access published on March 6, 2009

Requirement for *Shh* and *Fox* family genes at different stages in sweat gland development

Makoto Kunisada, Chang-Yi Cui*, Yulan Piao, Minoru S.H. Ko and David Schlessinger

Laboratory of Genetics, National Institute on Aging, National Institutes of Health, NIH Biomedical Research Center, 251 Bayview Boulevard, Suite 100, Baltimore, MD 21224, USA

Received December 12, 2008; Revised and Accepted February 20, 2009

Sweat glands play a fundamental role in thermal regulation in man, but the molecular mechanism of their development remains unknown. To initiate analyses, we compared the model of *Eda* mutant Tabby mice, in which sweat glands were not formed, with wild-type (WT) mice. We inferred developmental stages and critical genes based on observations at seven time points spanning embryonic, postnatal and adult life. In WT footpads, sweat gland germs were detected at E17.5. The coiling of secretory portions started at postnatal day 1 (P1), and sweat gland formation was essentially completed by P5. Consistent with a controlled morphological progression, expression profiling revealed stage-specific gene expression changes. Similar to the development of hair follicles—the other major skin appendage controlled by *EDA*—sweat gland induction and initial progression were accompanied by *Eda*-dependent up-regulation of the Shh pathway. During the further development of sweat gland secretory portions, *Foxa1* and *Foxi1*, not at all expressed in hair follicles, were progressively up-regulated in WT but not in Tabby footpads. Upon completion of WT development, *Shh* declined to Tabby levels, but *Fox* family genes remained at elevated levels in mature sweat glands. The results provide a framework for the further analysis of phased down-stream regulation of gene action, possibly by a signaling cascade, in response to *Eda*.

INTRODUCTION

Sweating is indispensable for the maintenance of human body temperature. In contrast to other mammals, whose sweat glands are few in number and restricted in distribution—in mice, exclusively in footpads—2–5 million sweat glands are distributed across the human body (1). As a dynamic secretory system, the cohort of sweat glands in one person produces up to 1–4 l of sweat per hour, a source of cooling in normal and feverish states (2).

Unsurprisingly, sweat gland absence or dysfunction can result in life-threatening hyperthermia. Such clinical concerns are uppermost for patients affected by anhidrotic/hypohidrotic ectodermal dysplasia (EDA), the most common form of EDs (OMIM 34500). In addition to complete lack of sweat glands, individuals with mutations in the *EDA* signaling pathway also have sparse hair and rudimentary teeth (reviewed in 3).

The mouse counterpart lacking an active *EDA* gene, Tabby, has revealed that *EDA* action extends further to additional skin appendages, including sebaceous, preputial, salivary, mammary and meibomian glands (4–7). Tabby mice thus provide an excellent model for studying exocrine gland development. It has been established that the *EDA* pathway, mediated by ligand ectodysplasin, receptor EDAR and receptor adaptor EDARADD, specifically activates NF-κB transcription factors for skin appendage development. Further detailed action of *EDA* has been explored mainly in hair follicles (6,8–10). To access the molecular dynamics of sweat gland development that involving direct and indirect targets of *EDA*, we analyzed the histological progression and accompanying gene expression changes in wild-type (WT) and Tabby mice. We report that as in hair follicles, *EDA*-dependent Shh signaling is critical for early stage sweat gland development. At later stages, *Fox* family transcription factors, Foxa1 and Foxi1, which are not detected in other skin appendages, are required for further development of sweat gland secretory segments. We have also identified other early sweat gland markers down-stream of *EDA* including keratin 79.

*To whom correspondence should be addressed. Tel: +1 4105588129; Fax: +1 4105588331; Email: cuic@grc.nia.nih.gov

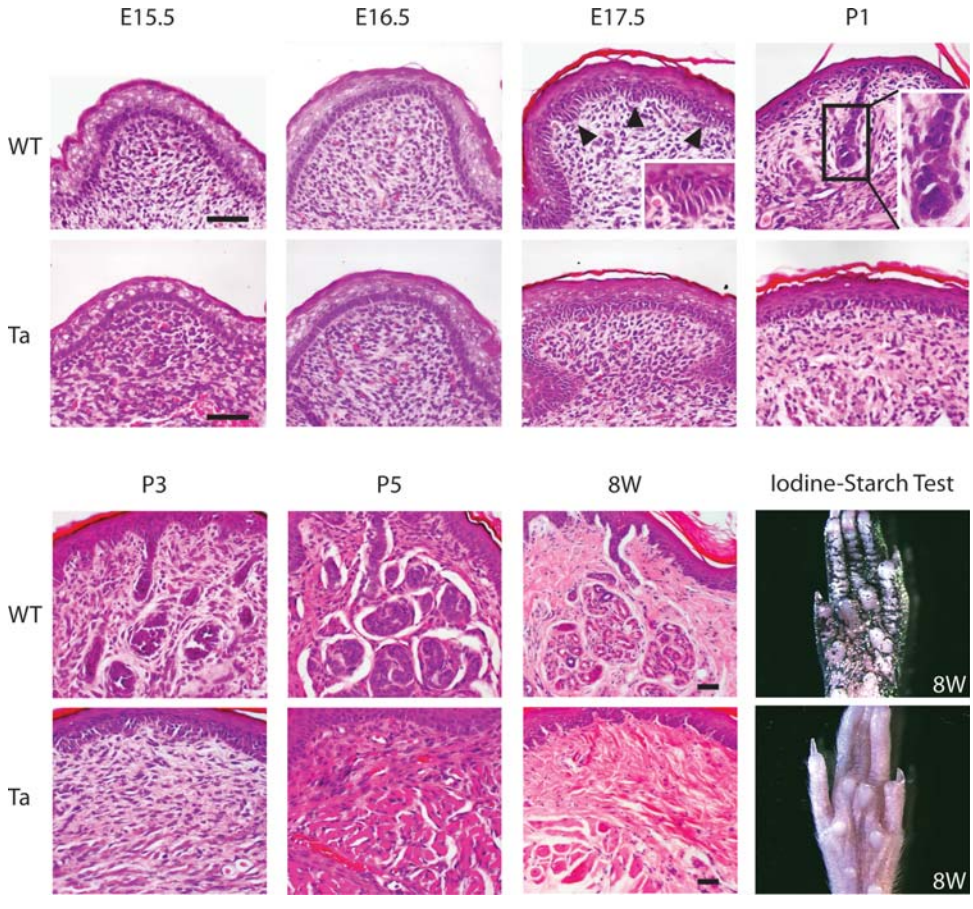

Figure 1. Time course of sweat gland development in mice. The general histology of WT and Tabby footpads at various developmental stages is shown. Sweat gland germs emerged at E17.5 (arrowheads) in WT mice. The sweat ducts started to coil at P1. The coiling, but not the central lumen formation, was essentially completed at P5. Sweat glands were not induced in Tabby footpads. Inserts in E17.5 and P1 show magnified sweat gland germs, and the start of sweat duct coiling. Scale bars, 50 μm.

RESULTS

Time course of sweat gland development in mice

Sweat glands comprise two major moieties, a ductal portion and a coiled secretory segment. During development, sweat gland germs emerge from the basal layer of epidermis and elongate downward into the dermis, where they form glandular globules. In man, sweat gland germs appear in the third month of gestation, start to coil at fourth month and complete development by eighth month in the palmoplantar skin (11,12). Sweat gland induction in the rest of skin area is delayed about 1 month in humans. To assess the appearance and timing of comparable developmental features in murine models, we studied the morphological progression of sweat glands in WT and Ta mice at embryonic days 15.5 (E15.5), E16.5 and E17.5, postnatal day 1 (P1), P3 and P5 and at 8 weeks (8W) (Fig. 1). No sweat glands or germs were seen in Ta at any stage, and the complete lack of sweating was confirmed by negative iodine–starch sweat test at 8W (Fig. 1). In WT, we found no histological indications of sweat gland induction at E15.5 or E16.5. The first sign of germ formation was observed at E17.5 in WT footpads, a cluster of basal cells protruding toward the mesenchyme (Fig. 1, arrowhead in E17.5). At P1, sweat gland germs grew downward and started to coil, forming secretory segments. This process was essentially completed by P5, when central lumen formation in the secretory segments was still apparent (Fig. 1). Thus, in contrast to the prenatal completion of sweat glands in man, sweat gland formation is completed after birth in mice.

Expression profiling revealed key genes involved in sweat gland development at different developmental stages

To define candidate genes critically involved at each developmental stage, we carried out gene expression profiling with RNAs from footpads at the seven developmental time points analyzed above (Fig. 1 and Supplementary Material, Fig. S1, which illustrates the sampling protocol). Notably, we found that in addition to sweat glands, there was some hair follicle formation in the center of hind footpads starting at P3. However, there was no hair follicle formation in fore footpads at any stage (Supplementary Material, Fig. S2 shows gross phenotypes and sample of histological sections). We therefore used only fore footpads for expression profiling of postnatal and adult mice.

To examine the overall transcriptome during WT sweat gland development, we analyzed the time course of trends of expression changes by principal component analysis.

Table 1. Shh and *Fox* family genes significantly down-regulated in Tabby footpads

Category	Time course of development						
	E15.5	E16.5	E17.5	P1	P3	P5	Adult (8W)
EDA pathway	*Eda*	*Eda*	*Eda*	*Eda* *Edar*	*Eda* *Edar*	*Eda* *Edar*	*Eda*
Shh pathway	*Shh*	*Shh*	*Shh* *Ptch1* *Ptch2*	*Shh*	*Shh* *Ptch1* *Gli1* *Hhip*	*Shh*	
Forkhead-box family				*Foxa1*	*Foxa1* *Foxc1* *Foxi1*	*Foxa1* *Foxc1* *Foxi1*	*Foxa1* *Foxc1* *Foxi1*

Genes down-regulated >1.5-fold in Tabby were listed at each time point.

Table 2. Keratin genes significantly down-regulated in Tabby footpads

Category	Time course of development						
	E15.5	E16.5	E17.5	P1	P3	P5	Adult (8W)
Epithelial keratins					*Krt8* *Krt18*	*Krt8* *Krt18* *Krt19*	*Krt8* *Krt18* *Krt19* *Krt23*
Hair follicle-related keratins	*Krt79*	*Krt79*	*Krt79*	*Krt79*	*Krt79* *Krt25* *Krt26* *Krt28* *Krt32* *Krt35* *Krt71* *Krt75*	*Krt79* *Krt25* *Krt26* *Krt27* *Krt28* *Krt32* *Krt35* *Krt71* *Krt75*	*Krt79*
Keratin-associated proteins						*Krtap5-1* *Krtap5-4* *Krtap9-1*	

Genes down-regulated >1.5-fold in Tabby were listed at each time point.

Consistent with a phased morphological progression, the analysis revealed three distinctive expression patterns: embryonic (E15.5–E17.5), postnatal (P1–P5) and adult stages (8W) (Supplementary Material, Fig. S3A). Approximately 70% of genes fall along the first principal component. They include *Foxa1, Krt79, Ptch1* and *Gli1*, all progressively up- or down-regulated during development, as further evidenced below. Another 20% of genes, including *Foxi1* and *Shh*, lie along PC2, showing sharp increase or decrease in adult animals (Supplementary Material, Fig. S3B).

In further analysis, when the expression of each gene was compared in WT and Ta to look specifically for *Eda*-dependent changes, a discrete but initially small set of genes stood out at each developmental stage of sweat gland germ formation. Overall, 11 genes were significantly different at E15.5, 17 at E16.5 and 20 at E17.5 (Supplementary Material, Table S1). The genes showing the most pronounced and consistent dependence on *Eda* expression included *Shh* and *Krt79*, but not other morphogens such as Wnts or Bmps (Tables 1 and 2). However, a greater number of genes were altered during the stages of secretory segment formation, 35 genes at P1, 152 at P3 and 219 at P5 (Supplementary Material, Table S1). In addition to *Shh*, *Fox* family transcription factors and a set of keratin genes including epithelial and hair follicle-related keratins were greatly altered at this stage (Tables 1 and 2). In adult animals, divergence increased, with 419 genes differentially expressed between WT and Ta (Supplementary Material, Table S1). Interestingly, by that time, *Shh* was down-regulated even in WT animals to the low level seen in Ta mice at the same stage. In contrast, the *Fox* family genes and epithelial keratins were continuously highly expressed in sweat glands, as detailed below.

Shh is involved as an *Eda* target in sweat gland development from induction to maturation, but not maintenance

To validate and more precisely quantify expression levels by an independent approach, we performed real-time PCR for selected genes. As expected, in WT footpads compared with Ta, *Eda* expression was itself significantly higher at all stages and its receptor *Edar* was moderately up-regulated from E17.5 until P5 (Fig. 2A).

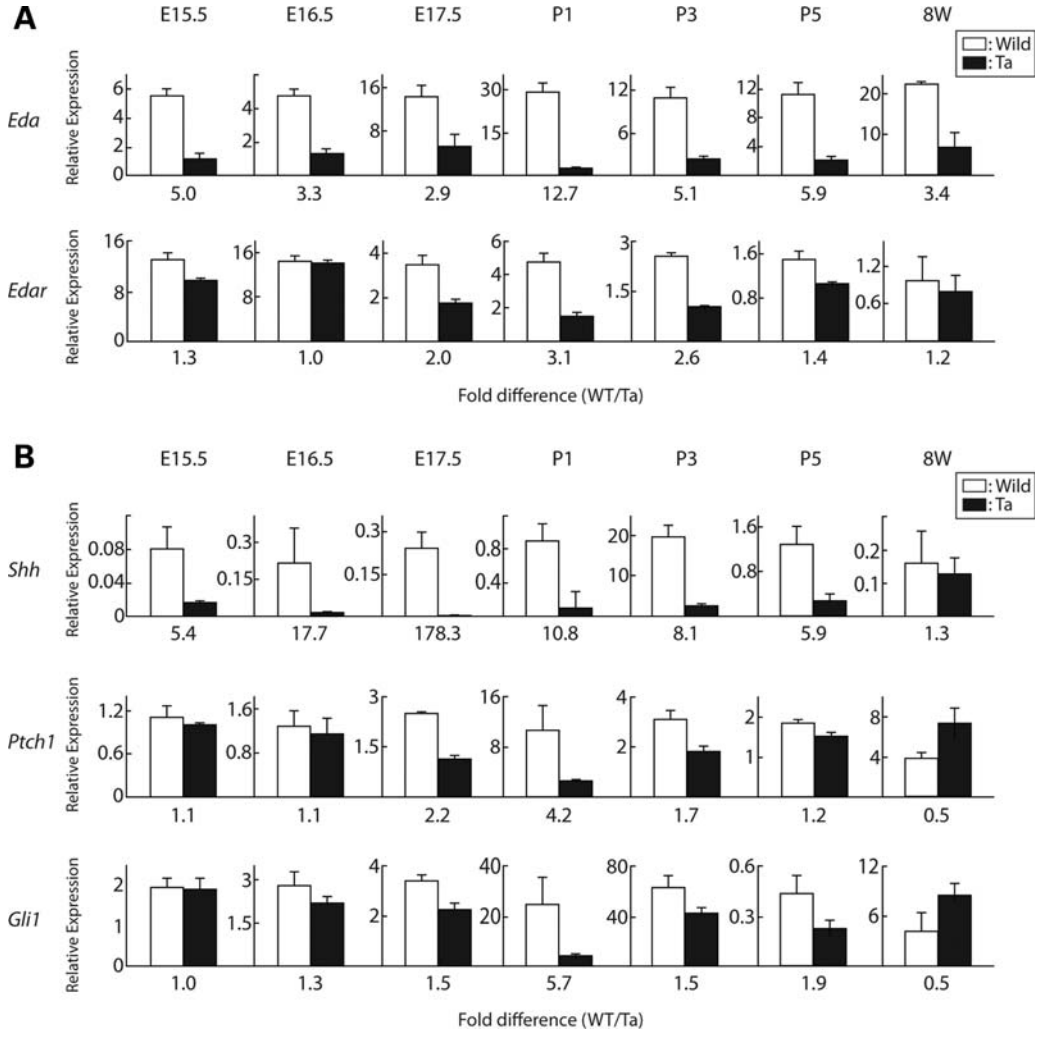

Figure 2. Expression levels of *EDA* and Shh pathway genes in WT and Tabby footpads. (**A**) *Eda* expression was significantly down-regulated in Tabby at all time points analyzed (upper panels). *Edar* was moderately down-regulated in Tabby during sweat gland germ induction and coiling stages (lower panels). (**B**) *Shh* was gradually up-regulated from E15.5, peaked at P3 and returned to a lower level at 8W in WT mice (upper panels, see scales on ordinate). *Shh* was dramatically down-regulated in Tabby in all developmental stages (upper panels). *Ptch1* and *Gli1* were significantly down-regulated in Tabby during the induction and coiling stages (middle and lower panels). Quantitative data are from real-time PCR assays.

Among the small numbers of genes significantly altered between WT and Ta during sweat gland germ formation, *Shh* was especially prominent, and was the only known morphogen detected (Supplementary Material, Table S1). *Shh* expression in WT footpads increased steadily from E15.5, peaked at P3 and then decreased back to the same level as in Ta at 8W, suggesting its involvement in development but not maintenance of sweat glands (Fig. 2B, *Shh*, scales on ordinate and Supplementary Material, Fig. S4). In contrast, *Shh* was sharply down-regulated in Ta footpads from E15.5, before sweat gland germ formation (Fig. 2B). Further dramatic down-regulation was seen at E17.5, when sweat gland germs were first detectable, and continued until completion of secretory portions at P5 (Fig. 2B). However, similar to observations in back skin (13), no difference was found for *Shh* expression in adult WT and Ta footpads (Fig. 2B). In further analyses, *Ptch1*, the *Shh* receptor (also a down-stream target), and *Gli1*, the down-stream transcription factor (23,24), were moderately down-regulated in Ta from E17.5 until P3 (Table 1 and Fig. 2B). *In situ* hybridization assays confirmed high expression of *Shh* in sweat gland germs in WT but not in Ta at E17.5 (Supplementary Material, Fig. S5). Thus, the expression patterns of *Shh* are very similar for sweat glands and hair follicles during development (9), and these results are all consistent with *Shh* as a key *Eda*-dependent effector for early stage sweat gland development.

Because Wnt has been shown to be an inducer of hair follicle development (14), we examined expression levels of Wnt pathway genes during sweat gland development. No significant expression changes were seen between WT and Ta in microarray profiles (Supplementary Material, Table S1). We carried out real-time PCR with probe/primers for *Wnt10b* and its antagonist *Dkk4*, which were significantly down-regulated in Ta skin during guard hair germ formation stage (9,15), and also checked *Lef1*, the transcription factor down-stream of Wnt. In agreement with the microarray results, no

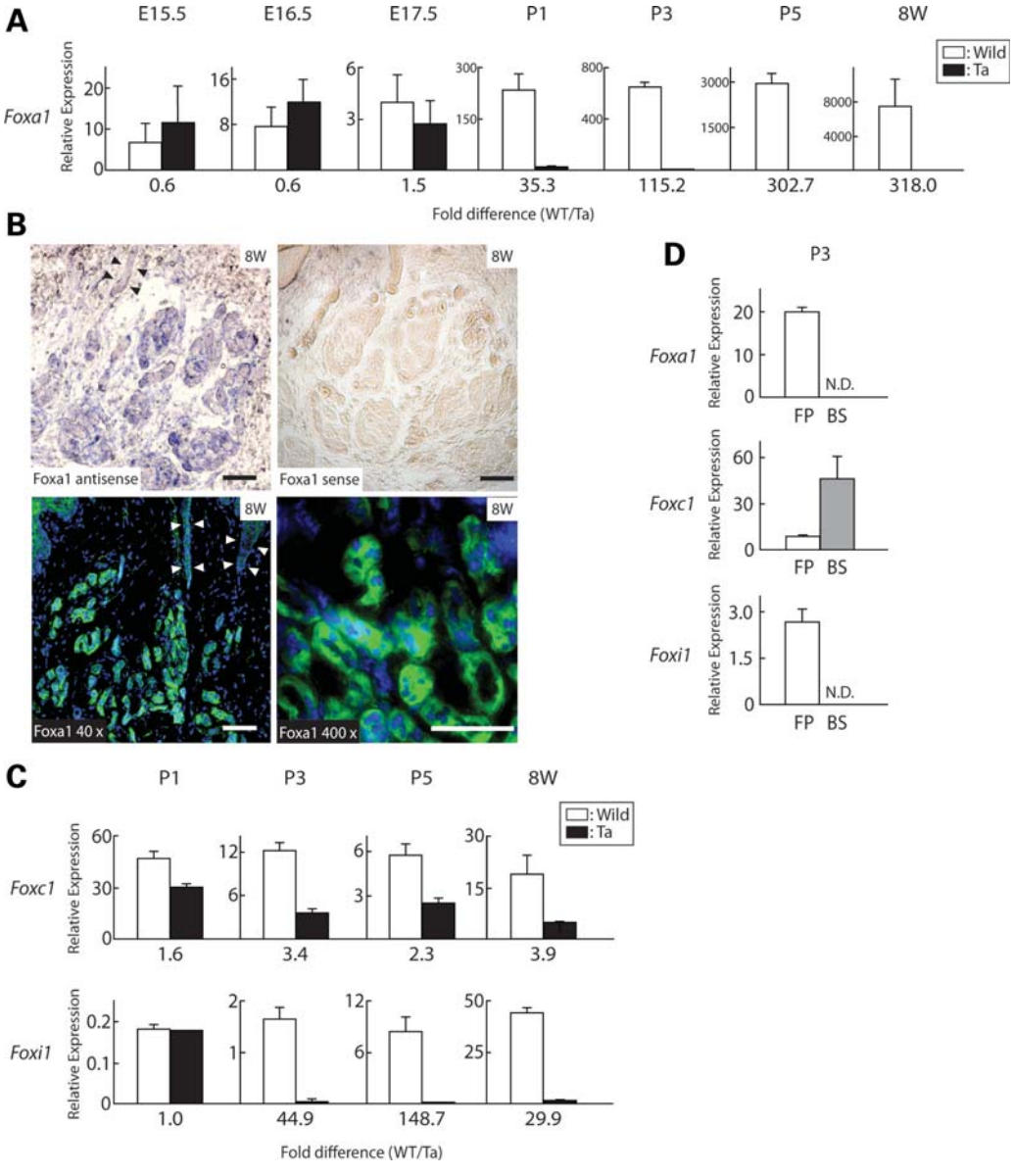

Figure 3. Expression patterns of *Fox* family genes in sweat glands. (**A**) *Foxa1* expression was up-regulated dramatically at P1 and progressively thereafter in WT footpads (see scales on ordinate), but not in Tabby. (**B**) *In situ* and immunofluorescent staining of Foxa1 in adult stage sweat glands. Foxa1 transcripts and proteins were expressed in the secretory portions of sweat glands, but not in the ductal segments (arrow heads). Scale bars, 50 μm. (**C**) Expression levels of *Foxc1* and *Foxi1* were significantly down-regulated in Tabby footpads from P3. (**D**) Expression levels of *Foxa1*, *Foxc1* and *Foxi1* in footpad skin (FP) and back skin (BS) at P3. *Foxa1* and *Foxi1* were specifically and highly expressed in footpads, but *Foxc1* expression was higher in back skin. N.D., not detected. Quantitative data are from real-time PCR assays.

expression changes were found for *Wnt10b* and *Lef1* between WT and Ta during sweat gland germ formation stage at E16.5 and E17.5, and a slight down-regulation of Dkk4 was seen in Tabby, but only at E17.5 (data not shown).

Involvement of *Fox* family transcription factors in later secretory gland development and adult sweat gland homeostasis

The up-regulation of *Fox* family transcription factor expression during secretory portion development and adult stage sweat gland homeostasis were unanticipated and obvious. *Foxa1* was sharply up-regulated from P1 to adult stage in WT mice (Fig. 3A, scales on ordinate, and Supplementary Material, Fig. S4). This coincided with the time at which sweat gland ducts started to form coiled secretory globules (Fig. 1). Surprisingly, in contrast to the 'early phase' gene *Shh*, *Foxa1* maintained high expression until adulthood, suggesting the involvement of *Foxa1* both in secretory segment formation and in homeostasis, and possibly sweating, of adult mice. Consistent with this possibility, *Foxa1* expression was sharply down-regulated in Tabby from P1 until 8W (Fig. 3A). *In situ* and immunofluorescent staining in adult stage WT sweat glands revealed specific

expression of Foxa1 in luminar cells of secretory portions rather than in ductal segments (Fig. 3B). Consistent with mRNA expression levels, Foxa1 protein was still low at P1, but was clearly discernible in secretory portions at P5 (Supplementary Material, Fig. S6).

Significant down-regulation of two other *Fox* family genes, *Foxc1* and *Foxi1*, in Tabby footpads was also seen from P3 through 8W (Fig. 3C).

To test whether *Foxa1*, *Foxc1* and *Foxi1* expressions were specific to sweat glands, we compared their expression levels at P3 between sweat glands containing footpads and hair follicle containing back skin by real-time PCR. *Foxc1* expression was much higher in back skin (Fig. 3D), so that it may have a more general role in skin appendage dynamics. However, in interesting contrast to footpads, neither *Foxa1* nor *Foxi1* expression was detected in back skin. This suggests that both are specific to sweat glands (Fig. 3D).

Notably, *Foxa1* has been shown to cooperate with *Foxa2* and *Foxa3* in liver and lung development (16,17). We therefore further examined the expression of *Foxa2* and *Foxa3* in WT and Tabby footpads at P1, P3, P5 and 8W by real-time PCR. However, unlike *Foxa1*, neither *Foxa2* nor *Foxa3* expression was affected in Tabby, suggesting their limited role in sweat gland development (Supplementary Material, Fig. S7A). We did note that *Foxa2* and *Foxa3* were nevertheless highly expressed in footpad skin compared with back skin, where their function remains to be further elucidated (Supplementary Material, Fig. S7B).

Keratin genes in sweat gland development

Significant down-regulation of many epithelial and hair follicle-related keratins in Tabby footpads was clear-cut. Among keratin genes, *Krt79* was progressively up-regulated in WT from E15.5 until 8W (Fig. 4A, scales on ordinate) and *Krt23* was up-regulated at only 8W (Table 2 and data not shown). Expression of *Krt79* was explored further. As expected for a gene directly or indirectly dependent on *Eda*, *Krt79* was significantly down-regulated in Tabby footpads from before sweat gland germ formation until adulthood (Fig. 4A), whose expression was found mainly in ductal portions of sweat glands at 8W (Fig. 4B).

Yet another member of the keratin, Krt77 (K1b), was previously reported as a sweat gland-specific marker, expressed in the luminal cells of sweat ducts (18). *Krt77* expression in WT footpads was much lower than *Krt79*, and its expression, assessed by microarray and real-time PCR assays (Supplementary Material, Fig. S8), was not significantly affected in Tabby mice. Thus *Krt77* may be a component of the footpad epidermis rather than an intrinsic component of sweat glands.

Expression profiling also revealed many keratins previously identified in epithelium, including *Krt8, Krt18* and *Krt19*, were down-regulated in Tabby footpads from P3 until 8W (Table 2). Unanticipated was the finding of >10 hair follicle-related keratins, and keratin-associated proteins that were significantly down-regulated in Tabby only at P3 and P5 (Table 2). For example, by immunohistochemistry, we detected expression of *Krt75*, already known to be associated with hair follicles (19). It was seen in myoepithelial cells of secretory portions in adult sweat glands (Fig. 4C). In a control experiment, we detected *Krt75* expression in companion layers—the innermost layer of the outer root sheath—of hair follicles in agreement with previous reports, but basal cells of epidermis were also positive (Fig. 4C). A role in sweat gland development for keratins that are also expressed in hair follicles suggests a common role for some keratin genes in the evolution of multiple skin appendages.

DISCUSSION

Gene expression profiling and confirmatory assays are consistent with Shh activation in a primary pathway initiated by *Eda* for sweat gland development at early stages, as it is in hair follicles and teeth (9). Thereafter, however, the fate choices involved in sweat gland down-growth and secretory coil formation diverge from the hair follicle model. Most striking is the sweat gland-specific activation of forkhead transcription factors, Foxa1 and Foxi1, accompanied by the formation of a number of keratins that include the idiosyncratic Krt79.

Shh in early stage sweat gland development

Shh was identified as a target of *EDA* for hair follicle development when the *EDA* signaling pathway was first established (20,21) and has been confirmed repeatedly (9,22). Shh was found to be dispensable for the induction of hair follicle germs, but required for down-growth of hair follicles (23,24). Its function in sweat gland formation is unknown, but it is progressively up-regulated from before sweat gland germ formation until the completions of secretory portions. *Shh* expression was dramatically down-regulated in footpads of Tabby mice throughout development. We infer that as in hair follicles, it has a morphogenetic role, consistent with significant down-regulation in Tabby mice of *Ptch1*, *Ptch2* and *Gli1*, the effectors of *Shh*.

Shh was the only morphogen seen among the few affected genes in Tabby in early stage sweat gland development. In contrast, at the time of guard hair germ formation, other morphogens such as Wnt10b and BMP4 were also down-regulated in Tabby mice (9,15,21). This suggests a greater degree or uniqueness of the Shh dependence of sweat gland development compared with hair follicles.

Notably, Shh nevertheless sharply declined in level upon the completion of sweat gland development whether or not *Eda* was expressed. The mechanism of *Eda*-independent regulation of Shh in mature sweat glands remains unknown, but its etiology may lie in an advantage gained by suppressing its potential oncogenic action (25).

Fox family genes in secretory portion development

Fox family transcription factors are involved in the development and maintenance of homeostasis in many organs (26). Four Fox family members were reported in skin appendages thus far. Mutations in *Foxq1* were reported to be responsible for satin mutant mice, in which hair shaft formation was aberrant (27). *FOXE1* expressed in the lower part of hair follicles is responsible for Bamforth–Lazarus syndrome that exhibits spiky and thinner hair in patients and mouse model (28).

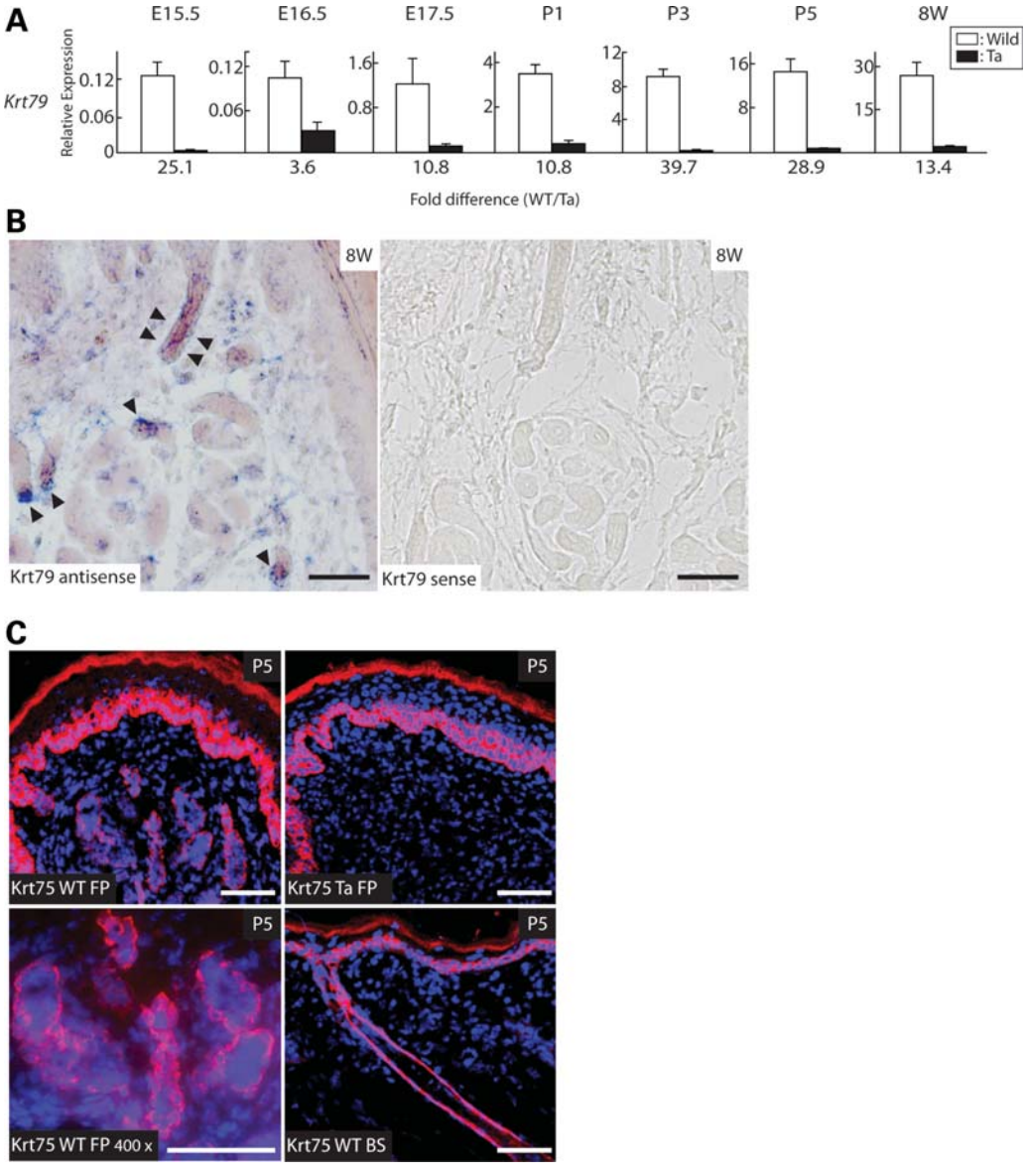

Figure 4. Expression of keratin genes in sweat glands. (**A**) *Krt79* expression was significantly down-regulated in Tabby footpads before, during and after sweat gland development. (**B**) *In situ* hybridization assay showed *Krt79* expression in ductal segments of sweat glands (arrowheads) in adult stage wild-type mice. Scale bars, 50 μm. (**C**) Krt75 was expressed in the myoepithelial cells of secretory portions in sweat glands, and the companion layers of hair follicles in P5 wild-type mice detected by immunofluorescent staining. Scale bars, 50 μm.

A *Foxi3* mutation was reported in hairless dogs and was speculated to be a target of *EDA* signaling (29). More recently, *FOXA2* was inferred to be a candidate gene responsible for male pattern baldness in some cases (30). Thus, increasing numbers of *Fox* family genes are being suggested as important in hair follicle dynamics.

This is the first finding of *Fox* gene activity in sweat glands. We identified five *Fox* family genes including *Foxa1, Foxa2, Foxa3, Foxc1* and *Foxi1*, none of which was reported to be expressed elsewhere in skin. *Foxa1* and *Foxi1* were not expressed in hair follicles, but were abruptly and progressively elevated during sweat gland secretory portion development and in adult sweat glands. They were, in fact, the most significantly affected genes in Tabby compared with WT at those stages. *Foxa1* and *Foxi1* expressions thus likely effect a strong divergence of hair follicle and sweat gland development, especially at late stages.

Given the late timing of their appearance, *Foxa1* and *Foxi1* may contribute to the development of secretory portions and/or maintenance of sweat production rather than induction of sweat glands. *Foxa1*, in particular, has already been reported to participate in lung and prostate ductal formation (17,31), and one can speculate that it may comparably promote the development of the secretory part of sweat glands.

Involvement of keratins in sweat gland development

It is increasingly apparent that rather than being a uniform, widely expressed gene cohort, keratins are assigned to precise locations and are often expressed at specific times.

As targets of *EDA* signaling in sweat gland development, we infer two findings concerning the involvement of keratins. First, *Krt79*, an epithelial keratin that appears unique to sweat glands, showed constant down-regulation in Ta footpads even before sweat gland germs appear; and other epithelial genes such as *Krt8*, *Krt18* and *Krt19* were down-regulated in Ta after P3, when the secretory portion was developing (18). Possibly *Krt79*, a down-stream target of *Eda* is a 'fundamental' structural marker for sweat glands. Until now, *Krt79* as well as *Krt23* have been labeled as having 'unknown localization' in compilations (32). Our data suggest that they can be regarded as sweat gland-specific keratins.

Secondly, and unexpectedly, several hair follicle-specific keratins were detected in mouse footpads, where no hair follicles have been observed. In particular, Krt75, which was known as a component of the companion layer in hair follicles, was detected in myoepithelial layers of the secretory portion of sweat glands. Interestingly, significant down-regulation of hair follicle keratins and keratin-associated proteins was restricted to P3 and P5 in Tabby mice, suggesting its spatio-temporal role in the development of sweat gland secretary portions. However, it cannot be excluded that these may also reflect illegitimate transcription products, with no real physiological role at P3–P5. Further analysis of the localization of these keratins within footpads/sweat glands and in mutant animal models should clarify whether they are intrinsic or adventitiously expressed proteins.

Overall, gene profiling has provided candidates for both regulation and structural differentiation of developing sweat glands. The *Eda–Shh* cascade appears to be involved in the initiation of sweat gland germs followed by the downward growth of the ducts. Later, they are joined by *Foxa1* and *Foxi1* during the development and function of secretory glands, whereas *Krt79* is constantly up-regulate in sweat glands, as illustrated in Figure 5. Although further analysis is needed to evaluate their functions, these genes become candidates for intrinsic roles specific to sweat gland development.

The relation of Foxa1 and Shh may be complex. For example, *Foxa1*-deficient mice showed higher levels of *Shh* in prostate epithelium, leading to hyper-proliferation and suggesting that *Foxa1* negatively regulates *Shh* (31). On the other hand, Wan *et al*. (17) reported that *Shh* mRNA was decreased after the deletion of *Foxa1* and *Foxa2*, and that lungs of *Shh* and *Foxa1* deficient-mice show a similar disruption of branching morphogenesis, suggesting that *Shh* is rather positively regulated by *Foxa1*. In our study, expression of *Foxa1* and *Foxi1* was preceded by Shh, more consistent with a *Shh–Foxa1/Foxi1* cascade. It remains to be seen whether *Shh* regulates *Foxa1* directly or whether the two genes work independently in the initiation and development of sweat glands.

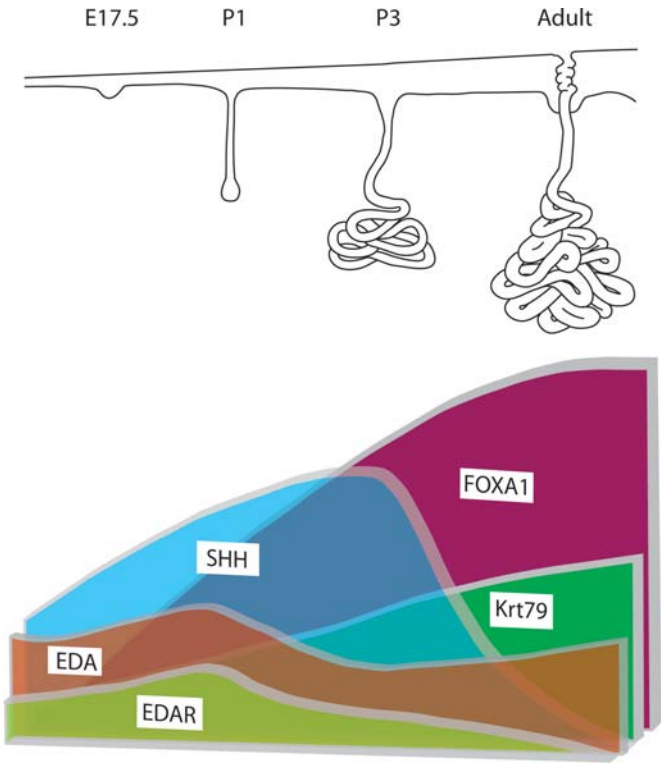

Figure 5. Schematic illustration of sweat gland development and accompanying expression changes of key genes. Upper panel, histological progression of sweat gland development in wild-type mice. Lower panel, *Shh* was progressively up-regulated during the induction and coiling stages, but was down-regulated in the adult stage. *Foxa1* expression was dramatically up-regulated during the coiling and maintenance stages, but not in the induction stage. *Krt79* was steadily up-regulated during development, and expression of *Eda* and *Edar* was up-regulated during induction and initial coiling stages.

MATERIALS AND METHODS

Timed mating and genotyping

Two sets of timed mating were set up. Ta male mice were crossed to Ta females [C57BL/6J/$A^{W-J}-Ta^{6J}$ (Ta)] (Jackson Laboratory, Bar Harbor, ME, USA); and WT C57BL/6J male mice were crossed to Ta females to have Ta hemi, homo, hetero and WT progeny. The morning after mating was designated as E0.5, and postnatal day 1 (P1) was equivalent to E20.5. Embryos and pups were harvested at E15.5, E16.5, E17.5, P1, P3, P5 and 8W. Footpads and livers were excised under dissection microscopy, immediately frozen on dry ice and stored at 80°C until use. Genomic DNA was isolated from each embryo liver using a DNeasy Tissue Kit (Qiagen, Valencia, CA, USA). Sex and *Eda* mutation status were assessed by PCR and subsequent restriction enzyme digestion based genotyping as previously described (9).

RNA isolation, gene expression profiling and real-time PCR

RNAs from fore- and hind-footpads (only fore-footpads for P1–8W) from each time point were used for microarray and real-time PCR analyses. The average numbers of footpads that yielded enough RNA (~30 μg) for a microarray/real-time PCR analysis for each genotype in each time point were 250 for embryos and 54 for postnatal pups. After genotyping, tissue samples were pooled into two separate groups for each genotype for biological replicates. RNAs were isolated according to previously described method (7), and cyanine-3-labeled cRNAs were generated and hybridized to the NIA Mouse 44K Microarray v3.0 manufactured by Agilent

Technologies (#015087) (33). Duplicate data were analyzed by ANOVA (34). Genes with FDR <0.1, fold difference >1.5 and mean log intensity >2.0 were considered to be significant.

One-step quantitative real-time RT–PCR with ready-to-use Taqman probe/primer sets (ABI Prism 7900 HT Sequence Detection System, Applied Biosystems, Foster, CA, USA) was performed to confirm microarray results. Analyzed genes by real-time PCR include *Eda, Edar, Shh, Ptch1, Gli1, Foxa1, Foxa2, Foxa3, Foxc1, Foxi1, Krt77, Krt79*. Total RNAs from back skin of E16.5 WT embryos were used to generate a standard curve. Each of the two groups of RNAs for WT and Ta was assayed in triplicate by real-time PCR. Reactions were normalized to GAPDH expression levels.

Histology, immunohistochemistry and *in situ* hybridization

For histological analyses, footpads from WT and Ta mice at each time point were fixed in 10% formaldehyde and embedded in paraffin; and 4 μm sections were then cut for hematoxylin/eosin staining (Sigma-Aldrich, St Louis, MO, USA). For immunofluorescent staining, anti-rabbit Foxa1 (1:10 dilution, Abcam, Cambridge, MA, USA) or anti-guinea pig Krt75 (1:100, PROGEN, Heidelberg, Germany) antibodies were incubated with 4 μm frozen footpad sections and then incubated with Alexa-fluor secondary antibodies (Invitrogen, Carlsbad, CA, USA) before applying 4′-6-Diamidino-2-phenylindole (DAPI) (Invitrogen). Samples were then analyzed by DeltaVision optical sectioning microscopy. For *in situ* hybridization, 12 μm frozen sections were fixed in 4% paraformaldehyde, incubated with proteinase K, and hybridized overnight at 60°C with a specific Digoxigenin (DIG)-labeled cRNA probe. After washing twice with 2× SSC (0.3 M NaCl and 0.03 M sodium citrate, pH 7.0) and twice with 0.1× SSC at 65°C, sections were incubated with anti-DIG antibody (1:500, Roche, Mannheim, Germany) overnight at 4°C and signals detected with NBT/BCIP solution (1:500, Roche). A full-length Shh cDNA clone was obtained from NIA mouse cDNA libraries (35); the *Eda-A1* cDNA was described previously (36); and *Foxa1* and *Krt79* cDNA clones were purchased from Open Biosystems (Huntsville, AL). DIG-labeled sense and anti-sense probes were prepared using a DIG RNA labeling kit (Roche). The length of probes was: 410 bp for *Shh* (nt 2101–2510 of BC063087.1), 381 bp for *Foxa1* (nt 2398–2779 of BC096524) and 540 bp for *Krt79* (nt 1511–2050 of BC031593).

SUPPLEMENTARY MATERIAL

Supplementary Material is available at *HMG* online.

ACKNOWLEDGEMENTS

We thank R. Nagaraja and V. Childress for technical assistance and critical reading of the manuscript; E. Douglass, A. Butler and M. Michel for help with animal housing and management.

Conflict of Interest statement. None declared.

FUNDING

This work was supported entirely by the IRP of the NIH, National Institute on Aging.

REFERENCES

1. Tsugane, M. and Yasuda, M. (1995) Dermatoglyphics on volar skin of mice: the normal pattern. *Anat. Rec.*, **242**, 225–232.
2. Hardy, J.D. (1961) Physiology of temperature regulation. *Physiol. Rev.*, **41**, 521–606.
3. Cui, C.Y. and Schlessinger, D. (2006) EDA signaling and skin appendage development. *Cell Cycle*, **5**, 2477–2483.
4. Cui, C.Y., Durmowicz, M., Ottolenghi, C., Hashimoto, T., Griggs, B., Srivastava, A.K. and Schlessinger, D. (2003) Inducible mEDA-A1 transgene mediates sebaceous gland hyperplasia and differential formation of two types of mouse hair follicles. *Hum. Mol. Genet.*, **12**, 2931–2940.
5. Jaskoll, T., Zhou, Y.M., Trump, G. and Melnick, M. (2003) Ectodysplasin receptor-mediated signaling is essential for embryonic submandibular salivary gland development. *Anat. Rec. A Discov. Mol. Cell Evol. Biol.*, **271**, 322–331.
6. Mustonen, T., Pispa, J., Mikkola, M.L., Pummila, M., Kangas, A.T., Pakkasjarvi, L., Jaatinen, R. and Thesleff, I. (2003) Stimulation of ectodermal organ development by Ectodysplasin-A1. *Dev. Biol.*, **259**, 123–136.
7. Cui, C.Y., Smith, J.A., Schlessinger, D. and Chan, C.C. (2005) X-linked anhidrotic ectodermal dysplasia disruption yields a mouse model for ocular surface disease and resultant blindness. *Am. J. Pathol.*, **167**, 89–95.
8. Fessing, M.Y., Sharova, T.Y., Sharov, A.A., Atoyan, R. and Botchkarev, V.A. (2006) Involvement of the *Edar* signaling in the control of hair follicle involution (catagen). *Am. J. Pathol.*, **169**, 2075–2084.
9. Cui, C.Y., Hashimoto, T., Grivennikov, S.I., Piao, Y., Nedospasov, S.A. and Schlessinger, D. (2006) Ectodysplasin regulates the lymphotoxin-beta pathway for hair differentiation. *Proc. Natl Acad. Sci. USA*, **103**, 9142–9147.
10. Cui, C.Y., Kunisada, M., Esibizione, D., Douglass, E.G. and Schlessinger, D. (2008) Analysis of the temporal requirement for Eda in hair and sweat gland development. *J. Invest. Dermatol*., October 16 (Epub ahead of print).
11. Hashimoto, K., Gross, B.G. and Lever, W.F. (1965) The ultrastructure of the skin of human embryos. I. The intraepidermal eccrine sweat duct. *J. Invest. Dermatol.*, **45**, 139–151.
12. Ersch, J. and Stallmach, T. (1999) Assessing gestational age from histology of fetal skin: an autopsy study of 379 fetuses. *Obstet. Gynecol.*, **94**, 753–757.
13. Cui, C.Y., Durmowicz, M., Tanaka, T.S., Hartung, A.J., Tezuka, T., Hashimoto, K., Ko, M.S., Srivastava, A.K. and Schlessinger, D. (2002) EDA targets revealed by skin gene expression profiles of wild-type, Tabby and Tabby EDA-A1 transgenic mice. *Hum. Mol. Genet.*, **11**, 1763–1773.
14. Millar, S.E. (2002) Molecular mechanisms regulating hair follicle development. *J. Invest. Dermatol.*, **118**, 216–225.
15. Andl, T., Reddy, S.T., Gaddapara, T. and Millar, S.E. (2002) WNT signals are required for the initiation of hair follicle development. *Dev. Cell*, **2**, 643–653.
16. Lee, C.S., Friedman, J.R., Fulmer, J.T. and Kaestner, K.H. (2005) The initiation of liver development is dependent on Foxa transcription factors. *Nature*, **435**, 944–947.
17. Wan, H., Dingle, S., Xu, Y., Besnard, V., Kaestner, K.H., Ang, S.L., Wert, S., Stahlman, M.T. and Whitsett, J.A. (2005) Compensatory roles of Foxa1 and Foxa2 during lung morphogenesis. *J. Biol. Chem.*, **280**, 13809–13816.
18. Langbein, L., Rogers, M.A., Praetzel, S., Cribier, B., Peltre, B., Gassler, N. and Schweizer, J. (2005) Characterization of a novel human type II epithelial keratin K1b, specifically expressed in eccrine sweat glands. *J. Invest. Dermatol.*, **125**, 428–444.
19. Wang, Z., Wong, P., Langbein, L., Schweizer, J. and Coulombe, P.A. (2003) Type II epithelial keratin 6hf (K6hf) is expressed in the companion layer, matrix, and medulla in anagen-stage hair follicles. *J. Invest. Dermatol.*, **121**, 1276–1282.

20. Kere, J., Srivastava, A.K., Montonen, O., Zonana, J., Thomas, N., Ferguson, B., Munoz, F., Morgan, D., Clarke, A., Baybayan, P. *et al.* (1996) X-linked anhidrotic (hypohidrotic) ectodermal dysplasia is caused by mutation in a novel transmembrane protein. *Nat. Genet.*, **13**, 409–416.
21. Headon, D.J. and Overbeek, P.A. (1999) Involvement of a novel Tnf receptor homologue in hair follicle induction. *Nat. Genet.*, **22**, 370–374.
22. Pummila, M., Fliniaux, I., Jaatinen, R., James, M.J., Laurikkala, J., Schneider, P., Thesleff, I. and Mikkola, M.L. (2007) Ectodysplasin has a dual role in ectodermal organogenesis: inhibition of Bmp activity and induction of Shh expression. *Development*, **134**, 117–125.
23. Chiang, C., Swan, R.Z., Grachtchouk, M., Bolinger, M., Litingtung, Y., Robertson, E.K., Cooper, M.K., Gaffield, W., Westphal, H., Beachy, P.A. *et al.* (1999) Essential role for Sonic hedgehog during hair follicle morphogenesis. *Dev. Biol.*, **205**, 1–9.
24. St-Jacques, B., Dassule, H.R., Karavanova, I., Botchkarev, V.A., Li, J., Danielian, P.S., McMahon, J.A., Lewis, P.M., Paus, R. and McMahon, A.P. (1998) Sonic hedgehog signaling is essential for hair development. *Curr. Biol.*, **8**, 1058–1068.
25. Epstein, E.H. (2008) Basal cell carcinomas: attack of the hedgehog. *Nat. Rev. Cancer*, **8**, 743–754.
26. Carlsson, P. and Mahlapuu, M. (2002) Forkhead transcription factors: key players in development and metabolism. *Dev. Biol.*, **250**, 1–23.
27. Hong, H.K., Noveroske, J.K., Headon, D.J., Liu, T., Sy, M.S., Justice, M.J. and Chakravarti, A. (2001) The winged helix/forkhead transcription factor Foxq1 regulates differentiation of hair in satin mice. *Genesis*, **29**, 163–171.
28. Brancaccio, A., Minichiello, A., Grachtchouk, M., Antonini, D., Sheng, H., Parlato, R., Dathan, N., Dlugosz, A.A. and Missero, C. (2004) Requirement of the forkhead gene Foxe1, a target of sonic hedgehog signaling, in hair follicle morphogenesis. *Hum. Mol. Genet.*, **13**, 2595–2606.
29. Drogemuller, C., Karlsson, E.K., Hytonen, M.K., Perloski, M., Dolf, G., Sainio, K., Lohi, H., Lindblad-Toh, K. and Leeb, T. (2008) A mutation in hairless dogs implicates FOXI3 in ectodermal development. *Science*, **321**, 1462.
30. Richards, J.B., Yuan, X., Geller, F., Waterworth, D., Bataille, V., Glass, D., Song, K., Waeber, G., Vollenweider, P., Aben, K.K. *et al.* (2008) Male-pattern baldness susceptibility locus at 20p11. *Nat. Genet.*, **40**, 1282–1284.
31. Gao, N., Ishii, K., Mirosevich, J., Kuwajima, S., Oppenheimer, S.R., Roberts, R.L., Jiang, M., Yu, X., Shappell, S.B., Caprioli, R.M. *et al.* (2005) Forkhead box A1 regulates prostate ductal morphogenesis and promotes epithelial cell maturation. *Development*, **132**, 3431–3443.
32. Moll, R., Divo, M. and Langbein, L. (2008) The human keratins: biology and pathology. *Histochem. Cell Biol.*, **129**, 705–733.
33. Carter, M.G., Hamatani, T., Sharov, A.A., Carmack, C.E., Qian, Y., Aiba, K., Ko, N.T., Dudekula, D.B., Brzoska, P.M., Hwang, S.S. *et al.* (2003) *In situ*-synthesized novel microarray optimized for mouse stem cell and early developmental expression profiling. *Genome Res.*, **13**, 1011–1021.
34. Sharov, A.A., Dudekula, D.B. and Ko, M.S. (2005) A web-based tool for principal component and significance analysis of microarray data. *Bioinformatics*, **21**, 2548–2549.
35. VanBuren, V., Piao, Y., Dudekula, D.B., Qian, Y., Carter, M.G., Martin, P.R., Stagg, C.A., Bassey, U.C., Aiba, K., Hamatani, T. *et al.* (2002) Assembly, verification and initial annotation of the NIA mouse 7.4K cDNA clone set. *Genome Res.*, **12**, 1999–2003.
36. Srivastava, A.K., Durmowicz, M.C., Hartung, A.J., Hudson, J., Ouzts, L.V., Donovan, D.M., Cui, C.Y. and Schlessinger, D. (2001) Ectodysplasin-A1 is sufficient to rescue both hair growth and sweat glands in Tabby mice. *Hum. Mol. Genet.*, **10**, 2973–2981.